DEVELOPMENT OF SMALL-SIZED SIDRA DEVICE FOR MONITORING OF CHARGED PARTICLE FLUXES IN SPACE

O. Dudnik [1,2], E. Kurbatov [1], J. Sylwester [3], M. Siarkowski [3], M. Kowalinski [3], V. Tarasov [4], L. Andryushenko [4], I. Zajtsevsky [5], E. Valtonen [6]

[1] Institute of Radio Astronomy, National Academy of Sciences of Ukraine (IRA NASU)
[2] V.N. Karazin Kharkiv National University, Ministry of Education and Science of Ukraine (KhNU)
[3] Solar Physics Division, Space Research Centre, Polish Academy of Sciences, Poland (SRC PAS)
[4] Institute for Scintillation Materials, National Academy of Sciences of Ukraine (ISMA NASU)
[5] Institute for Safety Problems of Nuclear Power Plants, National Academy of Sciences of Ukraine (ISPNPP NASU)
[6] Space Research Laboratory, Department of Physics and Astronomy, University of Turku, Finland

SIDRA rationale and objectives

Joint analyses of the data obtained with the help of Sphinx solar X-ray spectrophotometer and STEP-F satellite-borne telescope of electrons and protons on the board of the "CORONAS-Photon" satellite, showed a substantial difference in a character of electron energy spectra in the region of the South Atlantic Anomaly (SAA), and in the outer and inner radiation belts [1]. Observations have shown the evidence of presence of two inner electron radiation belts of the Earth magnetosphere at low altitudes even in case of weak geomagnetic storms [2]. The energy spectrum of particles found in the additional inner belt related to these storms, is considerably softer than that one of the main belt. In addition, the electron beams located below the radiation belts at the altitude of ~ 550 km demonstrate an expressed definite anisotropic character as compared to nearly isotropic distribution of particle fluxes of the SAA regions at similar altitudes. The results mentioned above were obtained during a quiet solar period covering a short time interval, and similar analysis needs to be extended in order to provide a more precise definition of physical characteristics of particles contained in the inner belt. In respect with this fact, further study of dynamics of electron fluxes and energy spectra has to continue.

The nature of electron micro-bursts generation in low and subequatorial latitudes below the Earth radiation belts, at the altitudes of several hundred kilometers from the Earth surface remains practically unexplored. Micro-bursts were unexpectedly detected in those zones of magnetosphere where they were not anticipated basing on the standard models of distribution of charged radiation, i.e. at low latitudes and close to the equator in the areas being far from SAA.

The conditions in the interplanetary plasma far from the Earth's magnetosphere, especially at the close distance to the Sun, are expected to be substantially different from that within the magnetosphere. There is great probability that high energy particles accelerated during solar flares, at the shocks of coronal mass ejections, associated with type II solar radio events and/or solar proton events are frequently being emanated from an active corona. These energetic particles carry important information on plasma parameters and processes in regions they are accelerated. Besides their passage or encounter with the satellite they pose substantial threat to the electronic systems of the spacecraft and the instruments onboard.

A compact telescope detecting high energy charged particles will work within the structure of X-ray spectrophotometer ChemiX with the purpose of alert in case the spacecraft enter the enhanced charged particle fluxes region, with the aim to take actions to protect sensors of the spectrophotometer from the destructive radiation doses during the "Interhelioprobe" interplanetary mission.

Composition and functional units of the device

Breadboard model of the SIDRA instrument (Satellite Instrument for Determination of Radiation environment) is shown in Fig. 1 [3—8]. The detector head is designed as a telescopic system consisting of 3 high-resistance silicon PIN-detectors of different thicknesses and an organic scintillation detector. Arranged directly below the detector head is an analog signal processing module. The module consists

of three indentical channels, comprising low noise charge sensitive preamplifiers, shaping amplifiers, scaling amplifiers, providing for programmable gain coefficients, as well as an separate shaping amplifier based channel. Additionally, the three signal processing channels comprise sample-and-hold circuits, as well as fast response analog-to-digital converters. The main tasks fulfilled by the signal digital processing module are collection and pre-processing of digital data obtained from the analog-to-digital converters, identification of types of particles and their energies, transmission of scientific data to the onboard computer [9].

The power module is positioned in the lower part of the instrument and consists of two identical semi-sets primary and spare assembled on the common printed circuit board. The module operates by the "cold redundancy" principle. The provisions are made for monitoring all secondary voltage values of both semi-sets with the help of the satellite telemetry system, as well as self-restored protective circuits are used in case of power module short-circuit failure condition. The protective circuits are provided both in the primary and redundant power supply circuits.

The PIN-detectors of the detector head are manufactured of super pure silicon. They are protected against direct solar illumination and low energy particles of interplanetary plasma with ~20 μm thick aluminum foil.

Fig. 2 depicts energy spectra of conversion electrons from ^{207}Bi β-radioactive source, recorded by D2 and D3 detectors using conventional laboratory equipment under normal temperature and humidity conditions. The spectra observed demonstrate rather high registration efficiency for the maximum energy of E_e= 1048 keV. In respect of D3 detector the registration efficiency is higher than that of D2, which is due to a larger thickness and, consequently, a larger quantity of electrons having been stopped completely in the detector crystal wafer. Good energy resolution ranging from ΔE = 14 keV to ΔE = = 17 keV for electrons, having energies in the range of E_e = 0.4—1 MeV, allows to implement the SIDRA instrument as an efficient charged particle energy spectrometer allowing for energy quantization step ΔE ≥ 20 keV.

The charge sensitive preamplifiers (CSA) are based on JFET input transistors and broadband operational amplifiers, with a feedback circuit, where the feedback capacitance C_f determines CSA sensitivity S_{CSA}, which is expressed in units mV/MeV. The shaping amplifiers are based on an active band pass filter which is provided by the baseline restoration circuits which operate efficiently with the pulse frequency rate in the range up to f = 250 kHz.

The scaling amplifiers controlled by sending appropriate commands from the onboard computer change the gain of analog spectrometric channels and the range of recorded energies. The range of output voltage U = 25—3600 mV determines the linear part of transfer characteristic $U_{out} = f(U_{in})$ of the analog signal processing sample-and-hold circuits in the spectrometric channels. The duration of shaping amplifier output pulse signals is ~2.1 μs at 0.1 U_{max} level, where U_{max} is the maximum amplitude of output signals. The sample-and-hold circuit feature wide range of duration of signals for holding, low distortions and the maximum count rate up to f = = 600 kHz. The maximum slew rate of peak detector signals is W = 8.1 V/μs.

Each channel of the analog signal processing module is provided with external connectors enabling to send test signals to the CSA inputs and to monitor the output signals of shapers and peak detectors am-

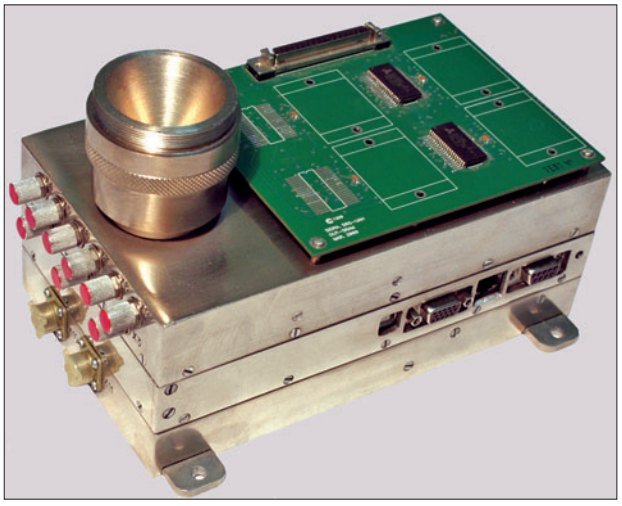

Fig. 1. Overall view of the SIDRA device breadboard model

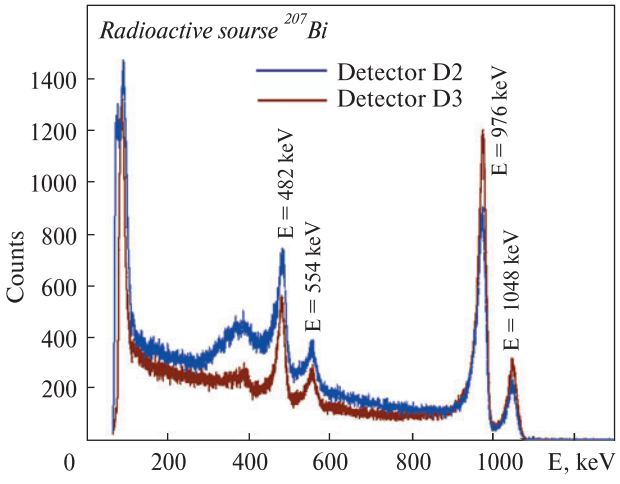

Fig. 2. Energy spectra of ^{207}Bi radioactive source electrons, registered by silicon detectors of the breadboard model of the SIDRA device

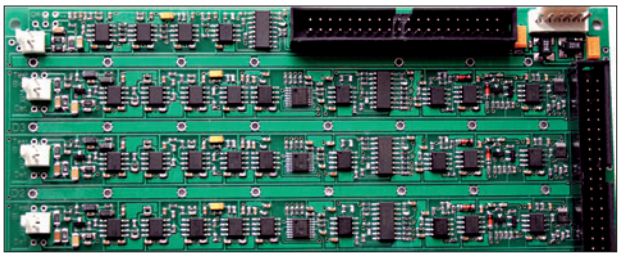

Fig. 3. General view of the signal analog processing channels of printed board from the side of component mounting

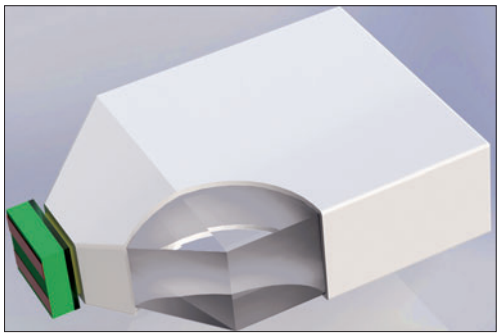

Fig. 4. Scintillation detector based on the para-terphenyl material, viewed by silicon photomultiplier of the SIDRA device breadboard model

plitude on the oscilloscope during the instrument adjustment. Fig. 3 shows a general view of signal analog processing channels of the printed circuit board from the side of component mounting.

Investigations of small-sized scintillators with standard geometric forms for choosing the anticoincidence detector of a telescopic system

With the aim of active protection of telescopic systems of satellite charged particle spectrometers the scintillators coupled with vacuum photomultiplier tubes (PMTs) are used quite often. These require high supply voltages, and have rather large dimensions; resistors of voltage dividers consume a lot of power and deliver high heat emission. The silicon photomultipliers (PMs), that are on par with vacuum PMTs in the sensitivity, have been started to be used recently more frequently. At the same time PMs have much smaller dimensions and weight in comparison with vacuum PMTs. In order to choose the form and the operation mode of the anticoincidence detector in the telescopic system of the SIDRA device breadboard model we accomplished the investigations of the performance and noise parameters of small-sized inorganic and organic scintillation detectors. The FEU-119 type vacuum PMT, the "Hamamatsu Photonics" S5106 silicon PIN photodiode with an active area of 5×5 mm^2 and the "Hamamatsu Photonics" silicon PM S10931-050P with an active area 3×3 mm^2 were used as photodetectors [10—12]. The scintillators used were stilbene, para-terphenyl, thallium-activated cesium iodide (CsI(Tl)) and polystyrene plastic scintillator. All of them were of cubic form with the volume of $10\times10\times10$ mm^3.

Measurements of the energy spectra of γ-rays from the radioactive isotope ^{137}Cs proved that when using the silicon PM with an active area of 3×3 mm^2, a satisfactory signal-to-noise ratio can be achieved with all the investigated scintillation detectors, including the plastic scintillator having low light output close to 5 photons per 1 keV of absorbed energy. Analysis of the noise characteristics of the detectors consisting of a CsI(Tl) crystal and the three different photodetectors showed that the noise energy equivalent for the vacuum photomultiplier was ≈4.1 keV, for the silicon PM ≈6.5 keV and for the large area PIN photodiode ≈64 keV. In addition to the high value of PIN photodiodes noise energy equivalent, the great disadvantage of their use is an effective simultaneous direct registration of γ-rays with energies of several tens of keV in experiments encountering mixed charge radiation, e.g., during the exploration of the near-Earth space. Investigation of the lightweight scintillation detector on the base of para-terphenyl as a candidate of the lowest detector in the SIDRA device telescopic system with the use of different photodetectors resulted in the value of the light output very close to the 27 photons per 1 keV of deposited energy. This satisfies the requirements for the anticoincidence detecting layer. As a result the form of detector with a light guide from the material of scintillator for light collection to the active area of multi pixel photon counter, represented in Fig. 4, has been chosen [13].

Computer simulation of the detector response on the particle passing

The GEANT-4 is a convenient program tool to perform the computer simulation of the response of the SIDRA prototype described above. In this respect GEANT-4 uses the Monte-Carlo approach. The architecture and various methods of GEANT classes' realization were developed. The model describes construction of the detector module, character of registered events, the order of saving the information obtained and methods of charge particle generation. As a result a mathematical model of the detector module in the GEANT-4-9.6.2 environment was obtained. It is suitable for modeling the response to high energy charged particles passing through a telescopic system of detectors as well as for visualization of primary and secondary particle tracks.

An analytic model has been created in several hardware configurations; the most perspective one includes three silicon detectors in the specially de-

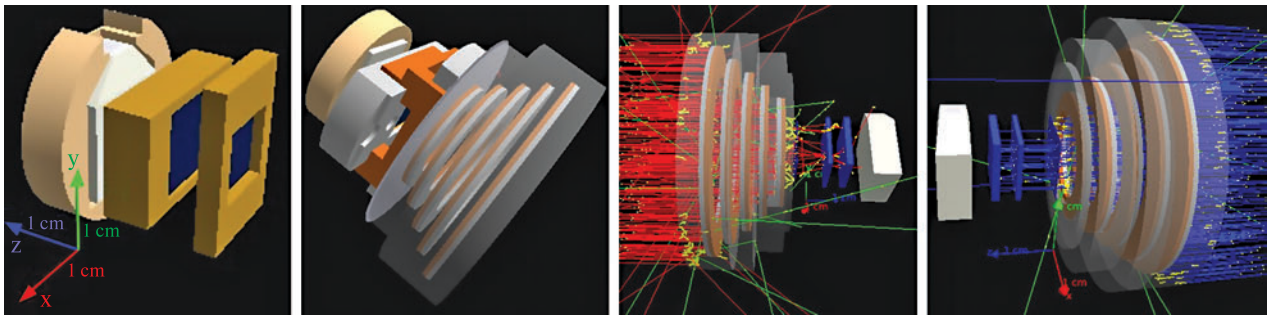

Fig. 5. Examples of visualization of the detector head analytic model, and of the particle tracks in case of their vertical incidence onto detector surfaces: electron tracks are shown in red and protons in blue. Tracks of secondary γ-quanta are shown in green, and δ-electrons are shown in yellow

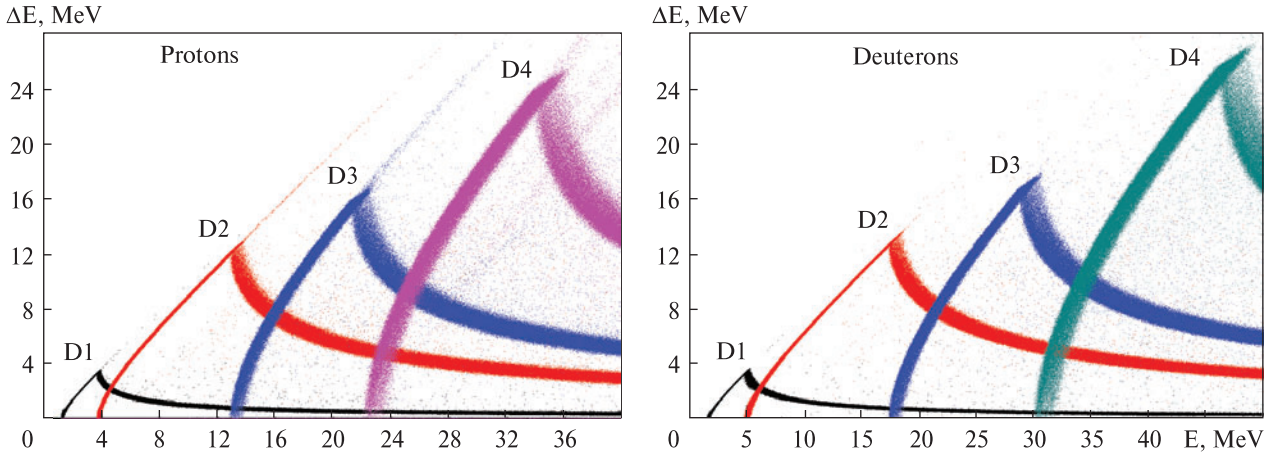

Fig. 6. Dependences of absorbed energies ΔE in each detector of the telescope versus proton and deuteron primary energies

Main specifications of the SIDRA breadboard model compared with similar parameters of SIXS, EPS и SEM-2 devices on BepiColombo, GOES и POES satellites

Specifications	SIDRA breadboard model	SIXS / BepiColombo	EPS / GOES	SEM-2 / POES
Mass, kg	<2.0	1.8	15.0	15.0
Dimensions, mm^3	205 × 145 × 135	366 × 208 × 145	No data	18.6×10^6
Power consumption at U = 27 V, Watts	<6	4.4	20.0	10.0
Output interfaces	Ethernet, serial, ESA	Serial, SpaceWire	No data	No data
Angle of view	~65°	5 telescopes, each 50°	Telescope: 70°, 3 dome, each 60°	2 × 15°, –x, –x + 90°
Active area of 1st detector, mm^2	100	4.9	Telescope: 100 dome: 25	25; 50
Types of particle detectors	Si (PIN), para-terphenyl scintillator	Si(PIN), CsI(Tl) scintillator	Si surface barrier, Si(PIN)	Si surface barrier, Si(PIN)
Energy ranges of registered particles, MeV	Electrons: 0.06÷2.4 Protons: 1.2÷14 Deuterons: 1.6÷18 Alpha-particles: 5÷52	Electrons: 0.1÷3.0 Protons: 1÷30	Electrons: 0.6÷4.0 Protons: 0.74÷900 Alpha: 3.8÷>500	Electrons: 0.03÷7.0 Protons: 0.03÷6.9 Protons: >16, >35, >70, 140
Number of energy channels	65 per each sort	8	16	Protons: 2 × 6 Electrons: 2 × 3 Protons omnidir.: 4
Time resolution, s	1, 10	1	3÷12	1, 2, 4
Telemetry rate, bits/s	~3400	~550	no data	160

signed metallic holders, scintillation detector covered with the light reflecting packing film, the box for detector module, and bimetallic stepped collimator Shown in Fig. 5 are the examples of visualization of the detector head of device's breadboard model that were performed using GEANT-4-9.6.2 medium as well as example of tracks of initially mono-energetic electron and proton beams.

The simulation of detector response to passing electrons, protons, deuterons and alpha-particles has been performed covering incident angle of ±42°, the quantity of primary particles for each sort of the particles with fixed energy was taken to be one million in every numerical exercise. The dependencies of energy losses as a function of particles primary energy in each telescopic detector layer were obtained in this way. Fig. 6 demonstrates dependencies of proton's and deuteron's absorbed energies in each detector versus their primary energy.

Prototype functionality validation and preliminary tests

The functionality of detectors and analog signal processing unit was tested with the use of radioactive isotopes and accelerated light-weight nuclei, which were produced at the cyclotron accelerator of the D.V. Skobeltsyn Institute for Nuclear Physics of the M.V. Lomonosov Moscow State University [7]. As the radioactive sources ^{207}Bi for energetic electrons, ^{226}Ra for α-particles and ^{241}Am for low energy γ-rays isotope sources were used. The cyclotron tests involved the use of accelerated beams of protons, deuterons and α-particles with energies up to 7.5 MeV/nucleon. Using a set of calibrated aluminum plates of different thickness placed in front of the detector, directed particle beams were produced, having energies up to E = 21 MeV. Combined calibration measurements, and results of numerical simulation by Monte-Carlo method are the source of initial data for design of signal processing logic and for microprocessor software development of device's digital data processing unit.

The thermal and vacuum tests of the SIDRA instrument breadboard model were carried out in the vacuum chamber at residual pressure of $P = (2—8) \times 10^{-5}$ Torr, the value of which depended on the rate of instrument breadboard model heating or cooling. The functionality of prototype was tested under the following conditions: 1) constant instrument mounting plate temperature maintained with the use of a cooling agent; 2) heating of the mounting plate up to the temperature +50 °C; 3) slow cooling down of the mounting plate to the temperature −34 °C. Prior to start the tests, special temperature sensors, i.e. calibrated thermocouples made of chromel—alumel alloys, were installed on the mounting plate surface in several positions: on the surface of field — programmable gate array (FPGA) Xilinx Spartan 3 XC3S1500 4FG456 and on the surface of secondary power board DC-DC converters radiator. The SIDRA instrument breadboard model has demonstrated its good functionality under deep vacuum conditions both in cases when the temperature of the mount plate was going down to the value of −34 °C, and when heating, going up to the temperature of +50 °C. We have found that by placing a special heat radiator to the surface of DC-DC converters we can reduce their temperature stresses. This solution will be applied in order to cool the FPGA surface.

Technical characteristics of the investigated breadboard model in the comparison with other satellite instruments

On the base of tests performed, measurements of electrical parameters, results of computer simulations with a help of GEANT4 toolkit and on the base of various supporting calculations we have defined main specifications of the SIDRA device breadboard model. In Table we present the results and data for the comparison with similar parameters of devices installed onboard BepiColombo, GOES and POES satellites.

REFERENCES

1. *Dudnik O.V., Podgorski P., Sylwester J., Gburek S., Kowalinski M., Siarkowski M., Plocieniak S., Bakala J.* X-Ray Spectrophotometer SphinX and Particle Spectrometer STEP-F of the Satellite Experiment CORONAS-PHOTON. Preliminary Results of the Joint Data Analysis // Solar System Research. — 2012. — V. 46. — No. 2. — P. 160—169.
2. *Dudnik O.* Unexpected behavior of subrelativistic electron fluxes under Earth radiation belts / 4th International workshop HEPPA/SOLARIS-2012 (9-12 October 2012, Boulder, Colorado, USA). — Abstract book. — P.15.
3. *Dudnik O.V., Prieto M., Kurbatov E.V., Sanchez S., Timakova T.G., Titov K.G., Parra P.* Small-Sized Device for Monitoring of High-Energy Electrons and Nuclei in the Outer Space // Space Science and Technology. — 2012. — V. 18. — No. 6. — P. 22—34 (in Russian).
4. *Dudnik O.V., Prieto M., Kurbatov E.V., Sanchez S., Timakova T.G., Spassky A.V., Dubina V.N., Parra P.* SIDRA Instrument for Measurements of Particle Fluxes at Satellite Altitudes. Laboratory Prototype // Solar System Research. — 2013. — V.47. — No.1. — P. 58—65.
5. *Prieto M., Dudnik O.V., Sanchez S., Kurbatov E.V., Timakova T.G., Tejedor J.I.G, Titov K.G.* Breadboard model of the SIDRA instrument designed for the measurement of charged particle fluxes in space // Journal of Instrumentation. — April 2013. — V. 8. — T04002.
6. *Dudnik O.V., Prieto M., Kurbatov E.V., Sanchez S., Titov K.G., Sylwester J., Gburek S., Podgorski P.* Functional capabilities of the breadboard model of SIDRA satellite-borne instrument // Problems of Atomic Science and

Technology. — 2013. — V. 3 (85) — Issue 60. — Series "Nuclear Physics Investigations". — P. 289—296.
7. *Dudnik O.V., Kurbatov E.V., Avilov A.M., Prieto M., Sanchez S., Spassky A.V., Titov K.G., Sylwester J., Gburek S., Podgorski P.* Results of the first tests of the SIDRA satellite-borne instrument breadboard model // Problems of Atomic Science and Technology. — 2013. — V. 3 (85). — Issue 60. — Series "Nuclear Physics Investigations". — P. 297—302.
8. *Dudnik O.V., Kurbatov E.V., Trefilova L.M., Andryushenko L.A., Tarasov V.O., Zajtsevskiy I.L.* Breadboard model of small-sized satellite instrument on the registration of energy charge particle fluxes / International Ukrainian-Japanese Conference on the scientific-industrial cooperation (24—25 October 2013, Odessa, Odessa National Polytechnic University, Ukraine). — Proceedings. —P.68—71.
9. *Dudnik O.V., Sanchez S., Prieto M., Kurbatov E.V., Timakova T.G., Dubina V.N., Parra P.* Onboardinstrument SIDRA prototype for measurements of radiation environment in the space / 39th Scientific Assembly of COSPAR. — July 14—22, 2012, Mysore, India). Abstracts. Session H0.3: "Technical Development of Instrumentation for Current Missions". — STW-B-153 H0.3-0023-12. — P. 106.
10. *Dudnik O.V.,Kurbatov E.V., Tarasov V.A., Andryushenko L.A., Boyarintsev A.Yu., Valtonen E.* Response and noise characteristics of small-sized inorganic and organic scintillation detectors measured with vacuum and solid-state photodetectors // Nuclear Instruments and Methods in Physics Research A. — 2012. — V. 664. — Issue 1. — P.148—153.
11. *Dudnik O.V., Kurbatov E.V., Valtonen E.* Amplitude and count rate characteristics of "Hamamatsu Photonics" multi pixel photon counters S10931-050P and S10931-100P // The Journal of Kharkiv National University. Physical series "Nuclei, Particles, Fields" No. 991. — 2012. — Issue 1(53). — P. 69—74 (in Russian).
12. *Dudnik O.V., Kurbatov E.V., Valtonen E.* Choice of bias voltages for silicon photomultipliers S10931-050P and S10931-100P // Problems of Atomic Science and Technology. Series "Nuclear Physics Investigations". — 2012. — No. 4 (80). — P. 210—215 (in Russian).
13. Patent of Ukraine № 86274, G01T 1/20. — Scintillation detector on the base of organic crystal — *Andryushenko L.A., Tarasov V.O., Grinyov B.V., Dudnik O.V., Kurbatov E.V.* — Declared 11.06.2013, No.U2013 07391. — Published. 25.12.2013. —Bulletin No. 24.